JOURNAL OF KUFA–PHYSICS
www.uokufa.edu.iq/journals/index.php/jkp | ISSN: 2077–5830

Preparation and Characterization of Organic-Inorganic Hybrid $MAPbI_2Br$ Perovskite

***Wadah Mohammed Mahdi** **Aref S. Baron**

Department of Physics, College of Science, University of Kufa, Al-Najaf, Iraq.

*Corresponding Author E-mail: wadahalasadi82@gmail.com

ARTICLE INF

Article history:
Received: 21 JUN, 2021
Revised: 02 AUG, 2021
Accepted: 18 AUG, 2021
Available Online: 10 DEC, 2021

Keywords:

Hybrid Perovskites
Methyl ammonium (MA)
Optical Properties
FESEM Observation

ABSTRACT

In this work, perovskite compounds were prepared and studied by using chemical methods for methyl ammonium halide MABr and lead halide PbI_2. The main objective of the study is to successfully prepare new types of perovskites using the one-step method by changing the weight ratios of lead halide PbI_2 in a fixed weight ratio of methyl ammonium bromide MABr, where they were classified into samples P_1 which represents $MABr/PbI_2$ weight ratios (0.22:0.39)g, P_4 which represents $MABr/PbI_2$ weight ratios (0.22:0.٥9)g and P_7 which represents $MABr/PbI_2$ weight ratios (0.22:0.79)g and the impact of this change was studied. High crystallinity was obtained in the crystal structure of the P_4 sample after increasing the weight ratio of lead halide from 0.39 g to 0.59 g. Then the crystallization decreased and the crystal structure changed after increasing the weight ratio from 0.59 g to 0.79 g in the sample P_7. The increase in PbI_2 weight from 0.39 g to 0.59 g and 0.79 g affected the absorption edge and shifted widely towards long wavelengths (red shift) from 625 nm to 691 nm and 805 nm. The energy band gap changed from 1.98 eV to 1.79 eV and to 1.53 eV. The study showed that the surface morphology of these samples, where a sample with a homogeneous film with a high density was obtained, resulted from an increase in the weight of lead halide from 0.39 g to 0.59 g and with small Nano-diameters of 34.25 nm for the P_4 sample. After increasing the weight from 0.59 g to 0.79 g, a sample was obtained with a less dense membrane that contains many voids and a semi-micro large particle diameter is 97.32 nm for the sample P_7. Finally, the sample P_4 was selected with good crystalline and optical properties and a homogeneous surface formation with a high density that could enter into the special composition for the manufacture of optical devices with high efficiency and stability.

DOI: http://dx.doi.org/10.31257/2018/JKP/2021/130201

تحضير وتشخيص $MAPbI_2Br$ بيروفسكايت هجين عضوي-لاعضوي

وضاح محمد مهدي عارف صالح بارون

العراق، النجف، جامعة الكوفة، كلية العلوم، قسم الفيزياء .

الـــخُـــلاصـــة:

في هذا العمل تم تحضير ودراسة مركبات البيروفسكايت من خلال استخدام الطرق الكيميائية لهاليد ميثيل الأمونيوم $MABr$ وهاليد الرصاص PbI_2. ان الهدف الرئيسي من الدراسة هو تم تحضير أنواع جديدة من البيروفسكايت بنجاح باستخدام طريقة الخطوة الواحدة بتغيير النسب الوزنية لهاليد الرصاص PbI_2 في نسبة وزنية ثابتة من بروميد ميثيل الأمونيوم $MABr$، حيث تم تصنيفها الى عينات P_1 الذي يمثل $PbI_2/MABr$ بنسبة وزنية ($0.39/0.22$)غم، P_4 الذي يمثل $PbI_2/MABr$ بنسبة وزنية ($0.59/0.22$)غم و P_7 الذي يمثل $PbI_2/MABr$ بنسبة وزنية ($0.79/0.22$)غم ودراسة تأثير هذا التغيير. تم الحصول على تبلور عالية في التركيب البلوري لعينة P_4 بعد زيادة نسبة وزن هاليد الرصاص من ٠.٣٩ غم إلى ٠.٥٩ غم. ثم قل التبلور وتغير التركيب البلوري بعد زيادة النسبة الوزنية من ٠.٥٩ غم إلى ٠.٧٩ غم في العينة P_7. ان الزيادة بوزن PbI_2 من ٠.٣٩ غم الى ٠.٥٩ غم والى ٠.٧٩ غم أثرت على حافة الامتصاص وتحولت على نطاق واسع نحو الأطوال الموجية الطويلة (التحول الأحمر) من ٦٢٥ نانومتر الى ٦٩١ نانومتر والى ٨٠٥ نانومتر. وتغيرت فجوة نطاق الطاقة من ١.٩٨الكترون فولت الى ١.٧٩الكترون فولت والى ١.٥٣الكترون فولت. أوضحت الدراسة أن التشكل السطحي لهذه العينات حيث تم الحصول على عينة ذات غشاء متجانس بكثافة عالية ناتج عن زيادة وزن هاليد الرصاص من ٠.٣٩ غم إلى ٠.٥٩ غم وقطر الجسيمات صغيرة نانوية هي ٣٤.٢٥ نانومتر لعينة P_4. وبعد زيادة الوزن من ٠.٥٩ غم إلى ٠.٧٩ غم تم الحصول على عينة بغشاء اقل كثافة ويحتوي على العديد من الفراغات وقطر الجسيمات كبير شبه مايكرو هي ٩٧.٣٢ نانومتر للعينة P_7. وأخيراً تم اختيار العينة P_4 بخصائص بلورية وبصرية جيدة وتشكل السطحي لها متجانس بكثافة عالية يمكن ان تدخل في التركيب الخاص لصناعة الأجهزة الضوئية بكفاءة واستقراريه عالية .

الكلمات المفتاحية:

بيروفسكايت هجين
ميثيل الأمونيوم(MA)
الخصائص البصرية
FESEM –

1. Introduction

Over the past ten years, great interest has been raised in organic-inorganic perovskites. which made them very important materials in industries such as transistors, sensors, photodetectors, and photoelectric cells [1,2]. This is because of their Tunable optical properties, High carrier mobility, surface deposition techniques, Low cost, and High efficiency [3,4]. In 1839 a German scientist Gustav Rose discovered during his journey in the Ural Mountains in Russia, a mineral consisting of CaTio3, classified it the Russian mineralogist Lev Perovsky which he named perovskite in 1792-1856 [5,6]. The prominent crystal structure of perovskite was first described by Victor Gold Schmidt in 1926. The scientist D. Weber in 1978 developed the first organic-inorganic perovskite in the original halide compound which methylammonium ions replaced the cesium cations. Perovskites are class of compounds which are represented by

the general chemical formula ABX_3. These materials in the A site perform a cation which is commonly organic such as methylammonium (MA) or formamidinium (FA) in the B site a divalent metal such as incor lead (Pb^{2+}) and tin (Sn^{2+}). And in the X site the metal ions are octahedrally coordinated by 8 halide anions (Cl^-, Br^-, I^-) as shown in figure1 [7,8]

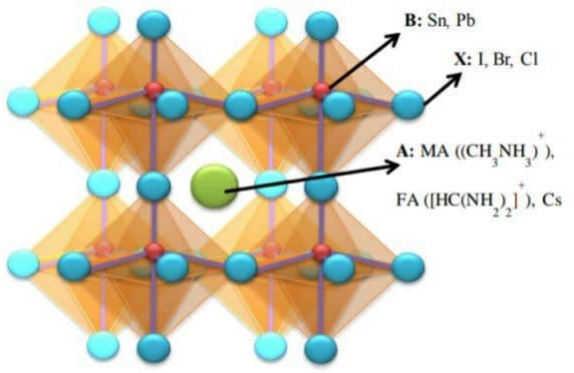

Figure 1. Perovskite ABX_3 structure [8].

Methylammonium lead halide perovskites $MAPbX_3$ (MA= methylammonium) CH_3NH_3 and (X=Br, Cl, I) hybrid organic-inorganic attention has recently increased with these structure in particular, which has a power bandgap that can be controlled by changing the cation or the metal or the halides.

Geometric tolerance factor (t)

The first description of the tolerance factor for perovskite was made by Victor M. Goldschmidt in 1926. Tolerance factor (t) is an indicator for the stability and distortion of crystal structures. It was originally only used to describe the Perovskite ABX_3 structure, but now tolerance factors are also used for ilmenite. Which is calculated based on the ratio of the ionic radii. It is the ratio of the (A–X) is $a/\sqrt{2}$ distance to the (B–X) is a/2 distance. The tolerance factor is given by the following relationship [9,10].

$$t = \frac{R_A + R_X}{\sqrt{2}\,(R_B + R_X)} \qquad (1)$$

R_A is the radius of the A cation, R_B is the radius of the B cation and R_X is the radius of the X anion.

2. Experimental Part

Materials

Methylammonium CH_3NH_2, Hydrobromied acid HBr, Diethyl ether $(C_2H_5)_2O$ (DEE), Lead nitrate $Pb(NO_3)_2$, Potassium iodide KI, Dimethyl formamide DMF, Ethanol, Acetone, Laboratory examination slides (WLD).

Preparation of Methylammoniom halide

MABr was synthesized according to reacting 9.2ml amethylammonium CH_3NH_2 with 14.6ml Hydrobromide acid HBr in a three neck round bottom flask was placed mixture down the ice bath about 0°C for 1h with stirring. A yellow mixture was obtained from CH_3NH_3Br (MABr) the mixture was turned into a powder by placing it on a drying system to evaporate at 60°C for an hour. MABr were washed with a Diethyl ether DEE (6) times. Then the powder was dried by evaporation at 80°C for 3h to obtain a powder from MABr [11,12]. As shown in figure 2(a).

Preparation of lead halides

PbI_2 were synthesized first, in which 2g of each of lead nitrate $Pb(NO_3)_2$ and potassium iodide KI were dissolved in 50ml of deionized water for each substance and then aqueous lead nitrate $Pb(NO_3)_2$ was mixed with aqueous KI. After a sediment was formed at the bottom of the beaker, and by means of a mixture filtration and drying process on the heating plate, a yellow powder of PbI_2 [11,12]. Was formed as shown in figure 2(b).

Perovskite Preparation

$MApbI_2Br$ was prepared in one step by mixing proportions of constant weights 0.223g of MABr with three different ratios (0.39,0.59 and 0.79)g of lead halide pbI_2 Each type of mixture was dissolved with Dimethyl Formamide (DMF) The solvent was heated at a temperature of 70°C for 1h with stirring[11]. The mixture was deposited on a glass plate with a spray system using a device (spin coating) as shown in figure 2(c).

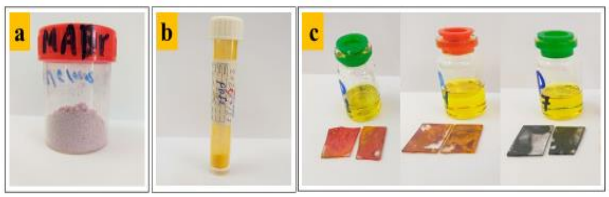

Figure 2. a) MABr powders, b) PbI_2 powders and c) kinds of films Perovskites $CH_3NH_3PbI_2Br$.

The precipitating film was annealed for 10min at 70^0 C to obtain a films of perovskite that was classified as P_1, P_4 and P_7 as shown in Table1. Which provides information about all Perovskite preparations in this study.

Table 1. The classification of perovskites $MAPbI_2Br$ Preparation

Sam-	Salt	Lead	Perovskite	Weight Salt (g)	Weight Lead (g)	Time (h)	Tem. (C^o)	Solution Color	Thin film Color
P_1	MABr	PbI_2	$MAPbI_2Br$	0.223	0.39	1	70	Light Yellow	dark Orange
P_4					0.59			yellow	Brown
P_7					0.79			yellow clear	Black

3. Result and Discussion

XRD Analysis

The X-ray characterizations of components of MABr and PbI_2 organic-inorganic which were prepared are very important to understand the behavior of the prepared perovskites by mixing two of these components in the one step method. For MABr, figure 3(a) shows the main peaks at 20.3°, 27.6°, 30.7°, 33.4°, 40.8°, 45.5°, and 52.2°. Indexed (110), (111), (200), (210), (220), (300) and (320) planes respectively. While figure 3(b) shows the behavior of PbI_2 with main peaks at 25.8°, 34.2°, 38.5°, 39.5°, 41.6°, 45.1°, 47.8°, 52.3° and 53.2° as in, indexed (111), (210), (211), (212), (220), (300), (310), (404) and (320) planes. This agrees with refs [13,14].

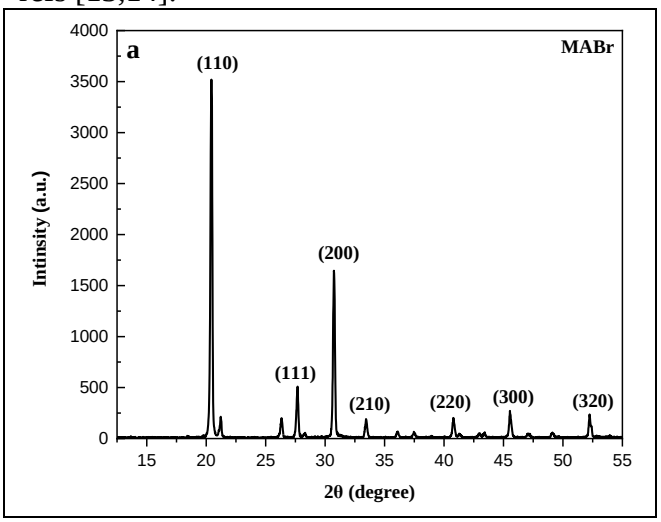

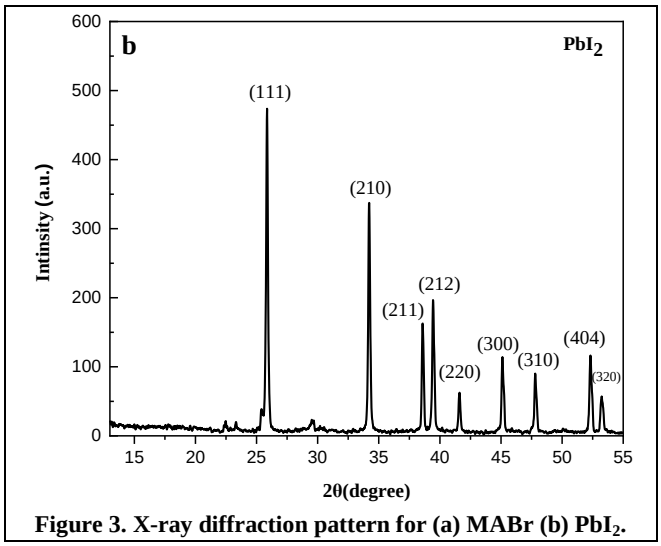

Figure 3. X-ray diffraction pattern for (a) MABr (b) PbI_2.

X-ray diffraction pattern was performed to investigate the crystalline structure for three types of $MAPbI_2Br$ perovskites P_1, P_4 and P_7. As shown in the figures 4, 5 and 6.

Figure 4 explains the X-ray diffraction pattern of P_1 which represents $MAPbI_2Br$ perovskite was prepared with weight ratios (0.22:0.39)g for $MABr/PbI_2$. The main peaks of this pattern at 14.9°, 16°, 28.7°, 30° and 41°. as indexed (100), (110), (200), (210) and (220). Which agrees with refs [15].

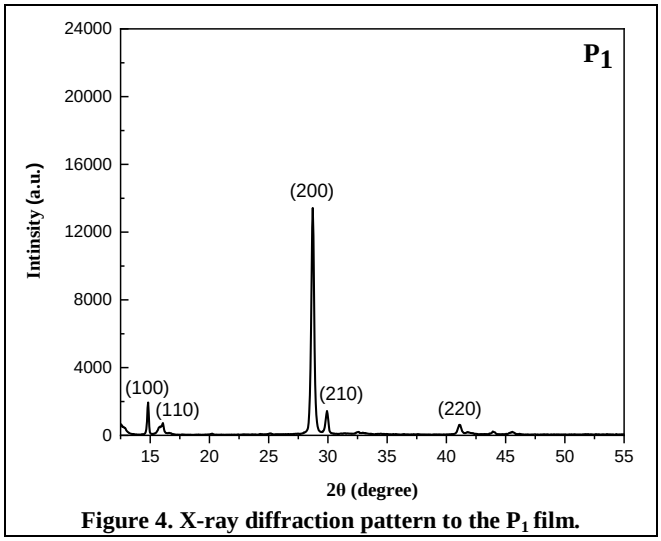

Figure 4. X-ray diffraction pattern to the P_1 film.

The X-ray diffraction pattern of P_4 explained in figure 5. This perovskite was prepared of with weight ratios (0.22:0.59)g for $MABr/PbI_2$. The main peaks of this pattern were at 14.9^o, 16^o, $28.7^{o,}$ 30^o and 41^o. As indexed (100), (110), (200), (210) and (220). The diffraction peaks of P_4 corresponds to P_1, but the XRD peaks intensity increases when PbI_2 was increased of P_4. This indicate for a high cubic crystal system, which agrees with refs [16,17].

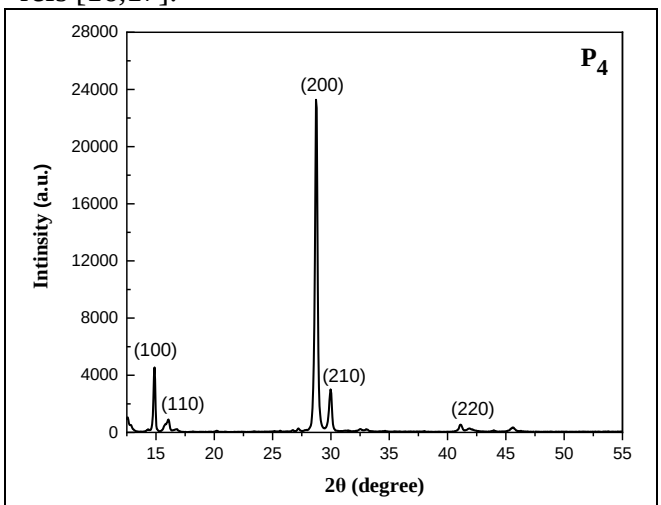

Figure 5. X-ray diffraction pattern to the P_4 film.

Figure 6 explains the X-ray diffraction pattern of P_7 sample. The prepared with weight ratios of (0.22:0.79)g for $MABr/PbI_2$. The main peaks of this pattern were seen at 14.3^o, 20.2^o, 24.8^o, 28.9^o, 32.3^o, 35.6^o, 41.3^o, 44^o and 51^o. As indexed (100), (110), (111), (200), (210), (212), (220), (300) and (320). It was observed that when lead halide was increased, the diffraction intensity decreased and the diffraction peaks increased. The peak at P_7 corresponds to the diffraction peak of perovskite $MAPbI_3$ the behavior of each directional tetragonal structure, this agrees with refs [17,18].

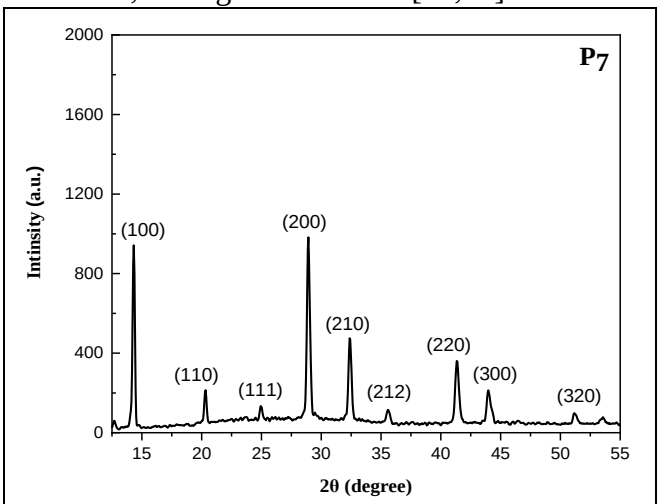

Figure 6. X-ray diffraction pattern to the P_7 film.

4. Optical Properties

For the UV-Visible absorption and photoluminescence study, prepared a films of the perovskite material deposited upon glass substrate. The band gap of the material is calculated by using formula:

$$E_g = 1237.5/\lambda \qquad (2)$$

where E_g is a band gap of the material and λ is the wavelength of absorption onset curve [19].

Figures 7, 8 and 9 showed the absorbance spectra perovskites $MAPbI_2Br$ for P_1, P_4 and P_7 samples. Increasing the PbI_2 weight ratios of the ratio of to MABr causes in affected the absorption edge shifting it widely towards long wavelengths (red shift) 625nm, 691nm and 805nm, and the energy gap changed 1.98eV, 1.79eV and 1.53eV. This agrees with refs [20,21].

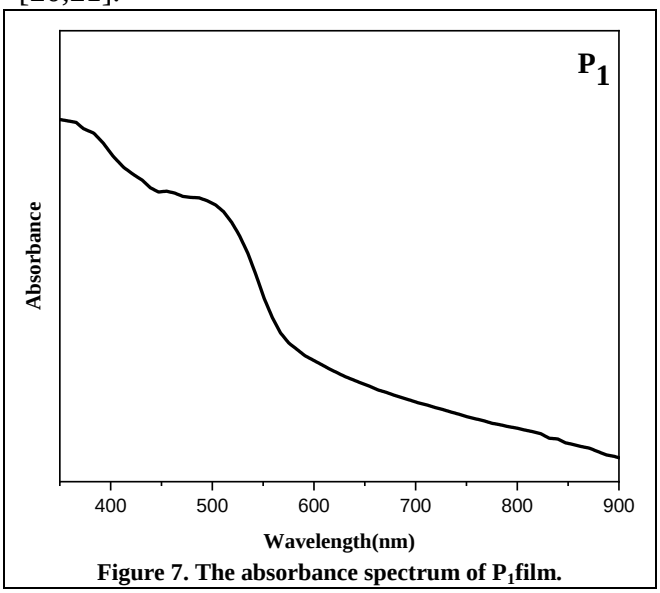

Figure 7. The absorbance spectrum of P_1film.

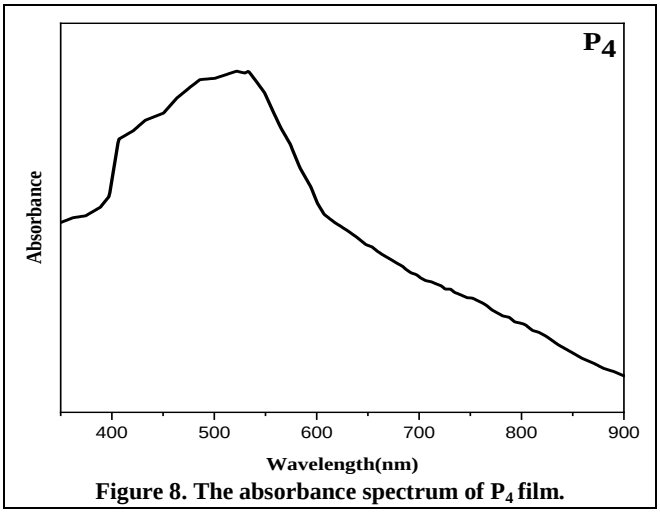

Figure 8. The absorbance spectrum of P_4 film.

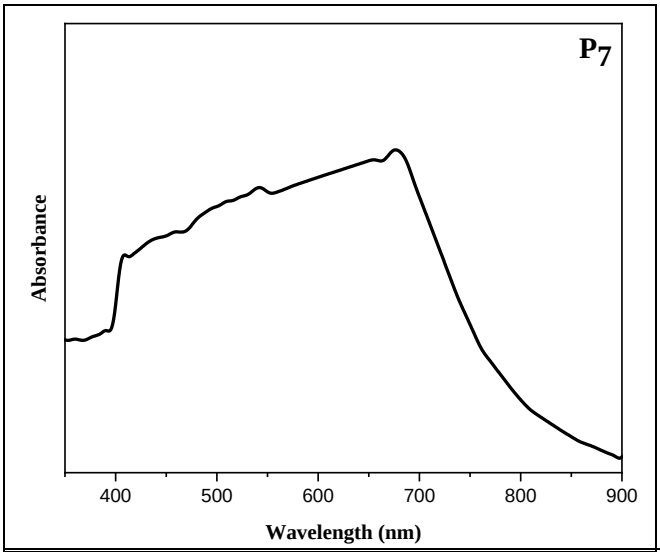

Figure 9. The absorbance spectrum of P_7 film.

FESEM images were used to provide information about surface morphology of the materials. The morphology of perovskites which prepared in the one step method (spin coating) on the glass. The precursor kind and ratios plays a critical role in determining the surface morphology and size.

The morphology of perovskites $MAPbI_2Br$ is shown in the Figures 10 (a), (b), (c) for P_1, P_4 and P_7 films, respectively. P_1 sample was small crystals that has a diameter of around 32-61nm. While increasing the ratios of the weight of PbI_2 the P_4 sample has diameter of around 34-54nm. It seemed denser and homogeneous. The perovskite P_7 has diameter of 97-190nm with many surface slits and it has a large size. This agrees with [22,23].

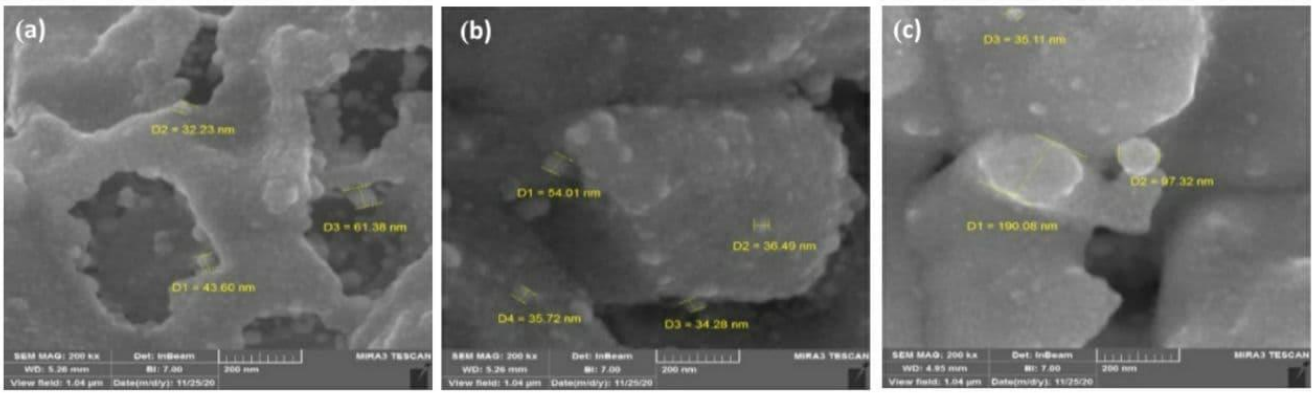

Figure 10. FESEM perovskites images (a) of sample P_1 (b) of sample P_4 (c) of sample P_7.

5. Conclusion

In this study, the organic-inorganic perovskite types were preparation and characterization after classification there to P_1, P_4 and P_7.

The effect of changing the weight ratios of lead halide on the kind of perovskite, by mixing MABr with three ratios of PbI_2 were studied.

The increase in the weight ratios of PbI_2 affected the absorption edge, shifting it towards long wavelengths (red shift) and reducing the energy bandgap.

Finally, the morphology of the deposition surface of the perovskite material was observed.

The type of perovskite P_4 appeared in the form of homogeneous nanoparticles with high density and continuous. It was possible to increase the efficiency and stability of perovskite.

Through tuning the band gap in perovskite by changing the weight ratio. It is very easy to fabricate active material in the manufacture of solar cell, optical sensors, light-emitting diodes, operating in wide wavelengths or any wavelength.

6. Acknowledgments

The authors are thankful to the Physics Department at the Faculty of Science, University of Kufa for their cooperation, and especially thank to Professor Dr. Adel H. Omran and Dr. Mohammad Malik Abood for assistance in completing this study.

7. References

[1] Agarkar, Shruti. "Dye sensitized solar cell: optimizing materials, methods and optoelectronic effects." (2014).

[2] Baron, Aref. S. "Synthesis and Characterization of methyl ammonium lead tri halide Perovskite Compounds and their Applications in Photonic Devices". University of Basrah (Doctoral dissertation, University of Basrah). Iraq (2019).

[3] Cai, Bing, Xing, Y., Yang, Z., Zhang, W. H., & Qiu, J. "High performance hybrid solar cells sensitized by organolead halide perovskites." Energy & Environmental Science 6.5, 1480-1485 (2013).

[4] H. Zhou, Q. Chen, G. Li, S. Luo, T. b. Song, H. S. Duan, Z. Hong, J. You, Y. Liu, and Y. Yang,"Interface engineering of highly efficient perovskite solar cells", Science, 345, 542-546, (2014).

[5] Baron, Aref S., Sattar J. Kasim, and Adel H. Omran. "Fabrication of a Solar Cells by Organic–Inorganic Hybrid Perovskites." EXECUTIVE EDITOR 9.12, 1276 (2018).

[6] Savage, Lynn. "Perovskite photovoltaics: hitting their stride." Optics and Photonics News 25.11, 26-33 (2014).

[7] Amu, Tochukwu Loreta. Performance optimization of tin halide perovskite solar cells via numerical simulation. Diss (2014).

[8] Brittman, Sarah, Gede Widia Pratama Adhyaksa, and Erik Christian Garnett. "The expanding world of hybrid perovskites: materials properties and emerging applications." MRS communications 5.1, 7-26 (2015).

[9] Salim, M., Chowdhury, M. S. H., Hossain, M. S., & Islam, M. A. "A micro-review on prospects and challenges of perovskite materials in organic-inorganic hybrid solar cell applications." Digest journal of nanomaterials and biostructures 10.4, 1289-1302 (2015).

[10] Zhang, Xiuwen, Stevanović, V., d'Avezac, M., Lany, S., & Zunger, A. "Prediction of A2B X4 metal-chalcogenide compounds via first-principles thermodynamics." Physical Review B 86.1, 014109, (2012).

[11] Bunaciu, A. A., UdriŞTioiu, E. G., X-ray diffraction: instrumentation and applications. Critical reviews in analytical chemistry, (2015).

[12] B. Roose, Engineering metal oxides for UV-stable perovskite solar cells, (2017).

[13] Ding, Jianxu, Zhao, Y., Du, S., Sun, Y., Cui, H., Zhan, X., ... & Jing, L. "Controlled growth of MAPbBr3 single crystal: understanding the growth morphologies of vicinal

hillocks on (100) facet to form perfect cubes." Journal of Materials Science 52.13, 7907-7916 (2017).

[14] Fu, Weifei, Yan, J., Zhang, Z., Ye, T., Liu, Y., Wu, J., ... & Chen, H. "Controlled crystallization of CH3NH3PbI3 films for perovskite solar cells by various PbI2 (X) complexes." Solar Energy Materials and Solar Cells 155, 331-340 (2016).

[15] Tumen-Ulzii, Ganbaatar, Qin, C., Klotz, D., Leyden, M. R., Wang, P., Auffray, M., ... & Adachi, C. "Detrimental Effect of Unreacted PbI2 on the Long-Term Stability of Perovskite Solar Cells." Advanced Materials 32.16, 1905035, 1905035 (2020).

[16] Wang, Huanhuan, Wang, Z., Yang, Z., Xu, Y., Ding, Y., Tan, L., ... & Luo, J. "Ligand-Modulated Excess PbI2 Nanosheets for Highly Efficient and Stable Perovskite Solar Cells." Advanced Materials 32.21, 2000865 (2020).

[17] Oku, Takeo. "Crystal structures of CH3NH3PbI3 and related perovskite compounds used for solar cells." Solar Cells-New Approaches and Reviews 1 (2015).

[18] Sutton, Rebecca J., Eperon, G. E., Miranda, L., Parrott, E. S., Kamino, B. A., Patel, J. B., ... & Snaith, H. J. "Bandgap-tunable cesium lead halide perovskites with high thermal stability for efficient solar cells." Advanced Energy Materials 6.8, 1502458 (2016).

[19] Gaya, Umar Ibrahim. Heterogeneous photocatalysis using inorganic semiconductor solids. Springer Science & Business Media (2013).

[20] M. Zhang, M. Lyu, H. Yu, J. H. Yun, Q. Wang, and L. Wang, "Stable and Low-Cost Mesoscopic CH3NH3PbI2Br Perovskite Solar Cells by using a Thin Poly (3-hexylthiophene) Layer as a Hole Transporter", Chemistry-A European Journal, 21, 434-439, (2015).

[21] L. Peng, Y. Hu, L. Xu, "Theoretical and Experimental Research on the Bulk Photovoltaic Effect in Hybrid Organic-Inorganic Perovskites CH3NH3PbI2 X (X= Cl, Br, I)", Science of Advanced Materials, 8, 2223-2230, (2016).

[22] Kumawat, Naresh K., Dhritiman Gupta, and Dinesh Kabra. "Recent Advances in Metal Halide-Based Perovskite Light-Emitting Diodes." Energy Technology 5.10: 1734-1749, (2017).

[23] Sarang, Som. Perovskite semiconductors: From high performance devices to optical characterization. Diss. UC Merced, (2019).